

# Multichannel quantum defect theory with numerical reference functions: Applications to cold atomic collisions

Dibyendu Sardar<sup>1,2</sup>, Arpita Rakshit<sup>3</sup>, Somnath Naskar<sup>1,4</sup> and Bimalendu Deb<sup>1\*</sup>

<sup>1</sup>*School of Physical Sciences, Indian Association for the Cultivation of Science, Jadavpur, Kolkata 700032, India.*

<sup>2</sup>*JILA, NIST, and Department of Physics, University of Colorado, Boulder, Colorado 80309-0440, USA.*

<sup>3</sup>*Engineering Institute For Junior Executive, Howrah-711104, INDIA.*

<sup>4</sup>*Department of Physics, Jogesh Chandra Chaudhuri College, Kolkata-700033, INDIA.*

We develop a method for the calculation of multichannel wavefunctions in the spirit of quantum defect theory using numerically calculated reference functions. We first verify our method by calculating cold collisional properties of  $^{85}\text{Rb}$  and  $^6\text{Li}$  in the presence of external magnetic fields tuned across specific  $s$ -wave Feshbach resonances and thereby reproducing known results. We then calculate recently discovered  $d$ -wave Feshbach resonance [Phys. Rev. Lett. **119**, 203402 (2017)] in  $^{87}\text{Rb}$ - $^{85}\text{Rb}$  cold collisions by our method. Our numerical results on this  $d$ -wave resonance agree reasonably well with the experimental ones. Our method is applicable to any arbitrary form of potentials and any arbitrary range of energies around threshold. The implementation of our method to any multichannel two-body scattering problem is straightforward.

## 1. INTRODUCTION

In recent times, cold atomic collisions have emerged as a key area of research, opening prospects for hitherto-unexplored regimes of cold chemistry [1, 2] where quantum correlations or entanglement can play an important role. One of the important methods for controlling the cold collisional properties of atoms is the magnetic Feshbach resonance (MFR) [3, 4]. Ever since its first experimental observation [5] in cold collisions of atoms two decades ago, MFR has remained an indispensable tool for tuning the  $s$ -wave scattering length. In fact, tunable MFR has been widely utilized in demonstrating a number of few- and many-body quantum effects using cold atomic gases [3, 6]. Apart from MFR, an optical method, known as optical Feshbach resonance (OFR) [7–10] that makes use of photoassociative coupling is currently being explored as an alternative tool for controlling interatomic interactions. Photoassociation (PA) [11, 12] is a photochemical process by which a pair of colliding cold atoms become bound into a molecule in an electronically excited state by a single photon absorption. Two-photon Raman photoassociation is being used to produce cold molecules in electronically ground state manifold. PA in the presence of an MFR can lead to Fano resonances [13, 14] which is a manifestation of quantum interference in spectroscopy or quantum collisions. At a fundamental level, all these resonances, namely, MFR, OFR and Fano resonances can be treated as a multichannel quantum scattering problem. Therefore, it is important to develop accurate but preferably simple and robust numerical method for solving a generic multichannel scattering problem.

The most accurate numerical method for solving multichannel quantum scattering problems is close-coupling (CC) method [15–17]. In this method, one needs to propagate wave functions in a matrix form outward starting from a short separation, and then match the functions with asymptotic boundary conditions. For an  $N$ -channel CC problem, each step of propagation requires an  $O(N^3)$  matrix operation, and so the usual CC algorithm takes a time proportional to  $N^3$ . Therefore, CC calculations are computationally very expensive. However, the properties of atomic and molecular collisions can also be calculated by several other methods which are computationally less expensive, among which the most important ones are the asymptotic bound-state model (ABM) [18, 19] and multichannel quantum defect theory (MQDT) [20]. In ABM method, one calculates only the bound states close to the thresholds of the channel potentials to describe low energy scattering properties like Feshbach resonance positions and scattering lengths bypassing the computation of explicit scattering states [18, 19]. Another important method is multichannel quantum defect theory (MQDT) which is the object of this study.

Historically, the ground work for quantum defect theory (QDT) was laid down by Seaton [20] in the context of collisions and spectroscopy of atomic Rydberg states, by considering the systematic separation of short and long-range parts of Coulomb potentials. Then, QDT was generalized to treat attractive or repulsive charge-dipole [21, 22] and polarization potentials [23–25]. This method has been successfully applied to scattering problems as diverse as negative ion photodetachment [23], predissociation of atom-diatom van der Waals complexes [26, 27] as well as diatomic molecules near threshold, hyperfine structure determination of molecular ions [28]. The prototype atom-molecule collision system  $\text{Mg} + \text{NH}$  has been dealt with MQDT [29]. Inelastic atomic scattering was analyzed by Mies [30] and Mies and Julienne [31] using MQDT method. In recent times, MQDT has attracted renewed interests for the treatment of ultracold atomic and molecular collisions [32–40]. A simple and efficient MQDT formalism was developed by Burke *et al* [33] using Milne phase-amplitude solutions for the calculation of magnetic Feshbach resonances of ultracold atoms. In a standard or semi-analytic MQDT method, the major task is to obtain a

---

\*REVTex Support: revtex@aps.org

matrix  $\mathbf{Y}$  [31, 34, 35] that completely describes the short-range dynamics and is almost insensitive to collision energy  $E$  and any external field such as magnetic field  $B$  in case of MFR. Once this matrix is deduced, one can use it for a relatively wide range of energies and fields. The time required for calculations at additional energies and fields is only proportional to  $N$  not  $N^3$ . MQDT method has been extended to calculate low energy atom-molecule chemical reactions with quantum state resolution [39] and ro-vibrational transitions in ultracold molecule-molecule collisions [40]. MQDT is also found to be quite useful for ion-atom cold collisions [41, 42]. The ion-atom and atom-atom potentials go as  $-C_4/r^4$  and  $-C_6/r^6$  as the separation  $r \rightarrow \infty$ , where  $C_4$  and  $C_6$  are the respective long-range dispersion coefficients. The analytical solutions of  $-C_6/r^6$  [43] and  $-C_4/r^4$  potentials have been employed to develop analytic MQDT methods by Gao [44, 45], giving much insight into ultracold atom-atom [46–49] and atom-ion [45, 50, 51] collision physics.

MQDT starts by propagating outward the multichannel wave function or its log-derivative in a matrix form from short separation. But, instead of propagating upto asymptotic region as in CC, the propagation is stopped at an intermediate and usually classically allowed separation known as matching point  $r_m$ . Then, this numerically obtained solution at  $r_m$  is matched with the analytical solutions of the long-range form of the potential matrix. Implicit assumptions or conditions in this method are that (i) for separations  $r > r_m$ , the off-diagonal elements of the potential matrix (which are basically inter-channel couplings) become negligible, rendering the potential matrix essentially into a diagonal form, and (ii) The diagonal elements of the potential matrix for  $r > r_m$  should be expressible, at least in leading order, in analytical forms that should also admit analytical solutions. The latter condition is the most stringent one, restricting the application of MQDT methods to certain specific classes of long-range potentials, such as Coulomb ( $1/r$ ), dipolar ( $1/r^2$ ), van der Waals ( $1/r^6$ ), charge-neutral ( $1/r^4$ ), etc. type potentials.

Here, we explore MQDT with a complete numerical approach for describing scattering phenomena in atomic systems. Our method comprises of two crucial steps. In the first step, we calculate some numerical reference functions taking different asymptotic or long-range boundary conditions of open and closed channels. We first calculate a reference function of a channel potential (which is a diagonal element of the potential matrix) considering an exponentially decaying or a sinusoidal function in asymptotic limit if the concerned channel is closed or open, respectively. Alternatively, one can utilize the analytical solution (if available) of the long-range part of the channel potential to set the appropriate boundary conditions at a long separation. We employ standard Numerov-Cooley procedure to calculate the function. We then calculate another reference function which is linearly independent to the former one by numerically solving the Wronskian equation for the two functions. The quantum defect functions are constructed by superposition of these two numerical reference functions. Then we perform an outward propagation in a matrix form up to a suitably chosen matching point in the classically allowed region. We then match this outward solution matrix with those numerically calculated quantum defect functions at the matching point using two point matching technique in the spirit of QDT. This matching procedure gives a short range matrix that we call as  $\mathbf{R}$  matrix. In second step, we carry out an asymptotic analysis to obtain physically acceptable solutions both for open and closed channels and finally we calculate scattering phase shift.

We apply our method to atomic collisions at low energy and calculate magnetic Feshbach resonances. First, to verify the effectiveness of our method, we calculate some known  $s$ -wave resonances of  $^{85}\text{Rb}+^{85}\text{Rb}$  and  $^6\text{Li}+^6\text{Li}$  systems. We then calculate  $d$ -wave magnetic Feshbach resonances of  $^{85}\text{Rb} + ^{87}\text{Rb}$  system. Recently, one broad  $d$ -wave Feshbach resonance in the hyperfine channel  $^{85}\text{Rb}| 2, -2\rangle + ^{87}\text{Rb}| 1, -1\rangle$  has been experimentally observed by You's group [49], who have interpreted the experimental results using a simplified two-channel model aided by the analytical quantum defect theory of Gao [43]. Here we carry out a 6-channel MQDT calculation using our method to derive the  $d$ -wave resonance of this system. In our calculations, we make use of the potential data as reported by Strauss *et al.* [56]. Our numerical results show that, in the absence of second order spin-spin interactions, the broad Feshbach resonance occurs at magnetic field of about 424.1 G and collision energy of 37  $\mu\text{K}$ . Experimentally, the broad Feshbach resonance was found at 423 G and temperature of 16  $\mu\text{K}$ . At lower temperature, one broad resonance peak splits into three narrower peaks due to spin-spin interaction. This triplet structure results from spin-spin couplings between open and closed channels corresponding to three magnetic sub-levels  $|m_{\ell=2}| = 0, 1, 2$  of the  $d$ -wave with transitions governed by  $\Delta m_{\ell} = 0$  [49]. When we include spin-spin interactions in our 6-channel all numerical MQDT calculation, we also find a triplet structure of the  $d$ -wave FR at lower energy. The peaks corresponding to  $|m_{\ell}| = 1, 2$  show increasingly larger positive shifts compared to that associated with  $m_{\ell} = 0$

In comparison to other MQDT methods, our method offers several advantages. First, our method is applicable to any arbitrary form of the long-range potentials unlike those MQDTs that use explicit analytical solutions of a select class of long-range potentials. Second, our method does not require any WKB-type boundary condition as in semi-analytical MQDTs in order to calculate pairs of reference functions. Third, our method guarantees that the numerically calculated pairs of reference functions remain absolutely linearly independent throughout the entire range. Fourth, real space Green function can be readily constructed using these linearly independent reference functions. So, the effect of any residual potential matrix can be taken into account as a final-state interaction by a perturbative approach, enabling more precise calculations of multichannel scattering wave functions. In passing, it is worth mentioning that the numerical reference functions have been previously computed by solving the Schrödinger equations subject to WKB type boundary conditions [40] considering the diagonal elements of the diabatic potential matrix.

The remainder of the paper is organized in the following way. In Sec. 2, we describe our numerical method for the calculation of reference functions and develop our all numerical MQDT. In Sec. 3, we verify our method by reproducing standard results of a two-channel model potential of  $^{85}\text{Rb}$  system and five channel  $^6\text{Li}$  system. Section 4 describes application of our method to

calculate higher partial-wave FR, in particular, the recently observed broad  $d$ -wave magnetic Feshbach resonances of  $^{85}\text{Rb}+^{87}\text{Rb}$  system in a particular incident channel. We present our results on the  $d$ -wave FR and compare them with the experimental observations of Ref. [49] in Sec. 5. Finally, in Sec.6 we conclude and make some remarks.

## 2. THEORETICAL APPROACH; NUMERICAL REFERENCE FUNCTIONS

In this section we describe the MQDT prescription based on numerical reference functions which are accurate enough to account for any kind of potential. A multichannel wave function for  $i$ th incident channel is expressed in the form

$$\Phi_i(r) = \sum_j F_{ji}(r) |j\rangle \quad (1)$$

where  $|j\rangle$  represents the channel state for  $j$ th channel. In the absence of any magnetic field, for a pair of ground-state atoms  $a$  and  $b$ , a channel state  $|j\rangle$  is defined as  $|j\rangle \equiv |(f_a f_b), f, \ell, J\rangle$  where  $f_{a(b)}$  is the hyperfine quantum number of the atom  $a(b)$ ,  $\mathbf{f} = \mathbf{f}_a + \mathbf{f}_b$  and  $\ell$  denotes the angular momentum (partial wave) of relative motion. Here  $\mathbf{J} = \mathbf{f} + \vec{\ell}$  is the total angular quantum number. In the absence of any external magnetic field,  $f$ ,  $\ell$  and  $J$  are quantum numbers. However, in the presence of an external magnetic field, none of these quantum numbers remains good enough except the total spin projection  $M_F = m_{s_a} + m_{i_a} + m_{s_b} + m_{i_b}$  and  $M_J = M_F + m_\ell$  along the quantization axis, where  $m_{s_{a(b)}}$  and  $m_{i_{a(b)}}$  are the projections of electronic spin  $s_{a(b)}$  and nuclear spin  $i_{a(b)}$ , respectively, of the atom  $a(b)$ ; and  $m_\ell$  is the projection of  $\ell$ . Here we have assumed that the rotational motion of internuclear axis is uncoupled or weakly coupled with the internal spin motion. In that case a channel is defined by diagonalizing the Hamiltonian of two non-interacting atoms including the atomic Zeeman shifts, resulting in a channel state which is a superposition of the product angular momentum states  $|(s_a i_a, m_{s_a} m_{i_a}); (s_b i_b, m_{s_b} m_{i_b})\rangle \otimes |\ell m_\ell\rangle$ . The full multichannel wave function can be conveniently expressed in a matrix form  $\Psi(r)$  whose  $i, j$  element is  $F_{ji}(r)$ .

Generally, time-independent coupled Schrödinger equations for the functions  $F_{ji}(r) \equiv F_j(r)$  (we suppress the second subscript  $i$  for simplicity) is given by

$$\left[ -\frac{\hbar^2}{2\mu} \frac{d^2}{dr^2} - E \right] F_j(r) + \sum_i W_{ij}(r) F_i(r) = 0 \quad (2)$$

where  $E$  is the collision energy and  $\mathbf{W}$  is the coupling matrix with elements

$$W_{ji}(r) = \int \psi_j^*(\tau) \left[ \hat{H}_{int}(\tau) + V(r, \tau) + \frac{\hbar^2 l_i(l_i + 1)}{2\mu r^2} \right] \psi_i(\tau) d\tau \quad (3)$$

Here  $\tau$  represents an internal degree-of-freedom of the system.  $W_{ji}(r)$  obeys the asymptotic behavior

$$W_{ji}(r \rightarrow \infty) \sim \left[ E_i^\infty + \frac{\hbar^2 l_i(l_i + 1)}{2\mu r^2} \right] \delta_{ij} + O(r^{-n}) \quad (4)$$

where  $l_i$  and  $E_i^\infty$  denote the partial-wave number and threshold of the  $i$ -th channel,  $n$  is the power of the leading term in the potential expansion and  $\mu$  is the reduced mass of colliding pair. In matrix representation, the Eq.2 becomes

$$-\frac{\hbar^2}{2\mu} \frac{d^2 \Psi}{dr^2} = [\mathbf{W}(r) - E\mathbf{I}] \Psi(r) \quad (5)$$

where  $\mathbf{I}$  is the identity matrix. For the calculation of scattering states and bound states, the wave function should vanish at the origin i.e the short-range boundary condition is

$$F_i(r) \rightarrow 0; \quad r \rightarrow 0 \quad (6)$$

For an  $N$ -channel problem, the above coupled equations yield  $N$  solution vectors that should satisfy boundary condition at  $r \rightarrow 0$  and form  $(N \times N)$  radial wave functions matrix  $\Psi(r)$ . In the following section, we describe our numerical method of MQDT in detail.

### 2.1. Inward propagation; solving Wronskian equation

Let there be  $N_o$  number of open channels which are enumerated starting from 1 to  $N_o$ , and  $N_c$  number of closed channels from  $N_o + 1$  to  $N$  with total channels being  $N = N_o + N_c$ . Initially, we calculate one solution  $\phi_i(r)$  of each channel  $i$  by inward

propagation of a standard single-channel Numerov-Cooley code starting from asymptotic limit up to the matching point  $r_m$ . Since the inter-channel mixing is negligible in this domain, independent single-channel propagation can be pursued. For a closed channel  $i$  the asymptotic boundary condition is set as

$$\phi_i(r \rightarrow \infty) \sim \exp(-\kappa_i r); \quad i = N_o + 1, \dots, N \quad (7)$$

where  $\kappa_i = \sqrt{W_{ii}(r \rightarrow \infty) - k^2}$  with  $k^2 = 2\mu E/\hbar^2$ . The point  $r_m$  is chosen in classically allowed region where the wavefunction  $\phi_i(r)$  crosses the first anti-node from outer side. For the open channels from  $i = 1$  to  $i = N_o$ , we consider sinusoidal asymptotic boundary condition  $\phi_i(r) \sim \sin(k_i r - \ell\pi/2)$  where  $k_i = \sqrt{k^2 - W_{ii}(r \rightarrow \infty)}$ . Once the function  $\phi_i(r)$  for each channel  $i$  is found, we calculate another solution  $\psi(r)$  by solving the Wronskian equation  $\phi_i'(r)\psi_i(r) - \psi_i'(r)\phi_i(r) = C$  where  $C = k_i$  if the channel is open or  $C = -2\kappa_i$  if it is closed. Although, the Wronskian equation (which is a first order inhomogeneous equation) admits an analytical solution [52], it is not of much use in practice as it can lead to numerical instability at or near the nodal points of  $\phi_i(r)$ . Instead, we solve this equation numerically to find the second solution  $\psi_i(r)$ . The numerical procedure for solving the Wronskian equation is discussed in appendix A.

For a closed channel  $i$ , we make linear combinations of these two linearly independent functions to obtain two new linearly independent functions which asymptotically go as sin and cosine hyperbolic functions. Let us denote this pair of functions as  $s_{c_i}$  and  $c_{c_i}$

$$s_{c_i}(r) = n_i(\phi_i(r) - \psi_i(r)) \quad (8)$$

$$c_{c_i}(r) = n_i(\phi_i(r) + \psi_i(r)) \quad (9)$$

where  $n_i = \sqrt{\kappa_i/\pi|E_i|}$  is the normalization constant (for energy normalization) with  $E_i = -\hbar^2 \kappa_i^2/2\mu$  being the asymptotic closed-channel energy. For an open channel  $i$  the corresponding pair functions are obtained by normalizing the functions  $\phi_i(r)$  and  $\psi_i(r)$  with the normalization constant  $n_i = \sqrt{k_i/\pi E_i}$  with  $E_i = \hbar^2 k_i^2/2\mu$ . We thus obtain desirable linearly-independent energy-normalized base pair or reference functions for both open and closed channels for building up our MQDT.

## 2.2. Outward propagation

Next, we calculate wave functions in matrix form by performing outward propagation from  $r \sim 0$  considering the short range boundary condition. For the  $N_c$  number of closed channels, the radial functions  $\mathbf{F}_{ij}(r)$  of the mentioned coupled Schrödinger equation will, in general, be exponentially rising in the large limit of  $r$ . But, the physical solutions should be bounded everywhere. These physically meaningful solutions can be constructed using radial functions  $\mathbf{G}_{ij}$  which satisfy the condition

$$\mathbf{G}_{ij}(r \sim \infty) \rightarrow 0 \quad (10)$$

where  $i = N_o + 1$  to  $N$ .

The diagonal elements  $G_{ii}$  or  $F_{ii}$  represents wave functions of the  $i$ -th channel whereas the off-diagonal terms  $G_{ij}$  or  $F_{ij}$  represents amplitude of transition between channel  $i$  and  $j$ . These functions can be partitioned as open-open ( $\mathbf{G}_{oo}$ ) and closed-open ( $\mathbf{G}_{co}$ ) counterparts following the work of Seaton [20]. Open-open components are  $\mathbf{G}_{ij}$  with  $i = 1$  to  $N_o$  and  $j = 1$  to  $N_o$ ; and for closed-open part  $i = N_o + 1$  to  $N$  and  $j = 1$  to  $N_o$ . The scattering reactance matrix  $\mathbf{R}$  is defined in terms of functions  $\mathbf{G}(\mathbf{R}; r)$  satisfying the asymptotic behavior for  $j = 1$  to  $N_o$  as

$$\mathbf{G}_{ij}(\mathbf{R}; r) \sim s_{o_i} \delta(i, j) + c_{o_i} \mathbf{R}_{ij} \quad \text{where } i = 1 \text{ to } N_o \quad (11)$$

$$\mathbf{G}_{ij}(\mathbf{R}; r) \sim 0 \quad \text{where } i = N_o + 1 \text{ to } N_c \quad (12)$$

where  $s_{o_i}$  and  $c_{o_i}$  represent the reference sine and cosine functions for open channels in asymptotic limit. In matrix notation

$$\mathbf{G}_{oo}(\mathbf{R}; r) \sim \mathbf{s} + \mathbf{cR} \quad (13)$$

$$\mathbf{G}_{co}(\mathbf{R}; r) \sim 0 \quad (14)$$

Finally, the numerically calculated wave functions obtained from outward propagation and reference functions of inward propagation are matched at a matching point  $r_m$  that lies in classically allowed region. The matching at  $r_m$  can be expressed as

$$\mathbf{F}(\mathcal{R}; r) = \mathbf{s} + \mathbf{cR} \quad \text{for } r \geq r_m \quad (15)$$

A complete set of solutions is described by a  $N \times N$  matrix  $\Psi(r)$  containing the elements  $F_{ij}(r)$ ,  $i = 1$  to  $N$  and  $j = 1$  to  $N$ . If  $\mathbf{F}_A(r)$  represents a particular complete set, the columns of any other set of solutions, say  $\mathbf{F}_B(r)$ , can be expressed as linear combinations of the columns of  $\mathbf{F}_A(r)$ . Therefore, we can say  $\mathbf{F}_B(r) = \mathbf{F}_A(r)\mathbf{C}$ , where  $\mathbf{C}$  does not depend on  $r$ .

### 2.3. Elimination of exponentially growing solutions of closed channels

In view of the above analysis, one can write

$$\mathbf{G}(\mathbf{R}; r) = \mathbf{F}(\mathcal{R}; r)\mathbf{L} \quad (16)$$

where the matrices  $\mathbf{L}$  have  $N_o$  columns and  $N$  rows. Consider the partitioning of  $\mathbf{F}(\mathcal{R}; r)$  into sub-matrices as

$$\mathbf{F} = \begin{bmatrix} \mathbf{F}_{oo} & \mathbf{F}_{oc} \\ \mathbf{F}_{co} & \mathbf{F}_{cc} \end{bmatrix}$$

where subscripts o stand for ‘‘open’’ and c for ‘‘closed’’. The sub-matrices  $\mathbf{F}_{oo}$ ,  $\mathbf{F}_{oc}$ ,  $\mathbf{F}_{co}$  and  $\mathbf{F}_{cc}$  are of dimensions  $N_o \times N_o$ ,  $N_o \times N_c$ ,  $N_c \times N_o$  and  $N_c \times N_c$ , respectively. Partitioning of  $\mathbf{L}$  is given as

$$\mathbf{L} = \begin{bmatrix} \mathbf{L}_{oo} \\ \mathbf{L}_{co} \end{bmatrix}$$

with  $\mathbf{L}_{oo}$  and  $\mathbf{L}_{co}$  are matrices of dimension  $N_o \times N_o$  and  $N_c \times N_o$ , respectively. From Eq.16, one can write

$$\mathbf{G}(\mathbf{R}) = \begin{bmatrix} \mathbf{F}_{oo}(\mathcal{R})\mathbf{L}_{oo} + \mathbf{F}_{oc}(\mathcal{R})\mathbf{L}_{co} \\ \mathbf{F}_{co}(\mathcal{R})\mathbf{L}_{oo} + \mathbf{F}_{cc}(\mathcal{R})\mathbf{L}_{co} \end{bmatrix}$$

Using Eq.15 for  $r \geq r_m$

$$\mathbf{G}_{oo}(\mathbf{R}) = s_o\mathbf{L}_{oo} + c_o(\mathcal{R}_{oo}\mathbf{L}_{oo} + \mathcal{R}_{oc}\mathbf{L}_{co}) \quad (17)$$

$$\mathbf{G}_{co}(\mathbf{R}) = s_c\mathbf{L}_{oo} + c_c(\mathcal{R}_{co}\mathbf{L}_{oo} + \mathcal{R}_{cc}\mathbf{L}_{co}) \quad (18)$$

$\mathbf{L}$  should be taken such that Eq.13 is satisfied. Comparing Eq.13 and Eq.17, we get

$$\mathbf{L}_{oo} = 1 \quad (19)$$

and

$$\mathbf{R} = \mathcal{R}_{oo} + \mathcal{R}_{oc}\mathbf{L}_{co} \quad (20)$$

Eq.14 is satisfied if the coefficient of the exponentially growing term is equated to zero,

$$\mathbf{L}_{co} = (1 - \mathcal{R}_{cc})^{-1}\mathcal{R}_{co} \quad (21)$$

Substituting  $\mathbf{L}_{oo}$  from Eq.21 into Eq.20 we get the final expression of  $\mathbf{R}$  which is the same as the familiar  $\mathbf{K}$  matrix of scattering theory. The scattering  $S$ -matrix is given by  $\mathbf{S} = (\mathbf{1} - i\mathbf{K})^{-1}(\mathbf{1} + i\mathbf{K})$ . We define the scattering  $\mathbf{T}$  matrix by  $\mathbf{T} = \mathbf{1} - \mathbf{S}$ .

## 3. VERIFICATIONS

To verify whether our proposed method as described above works well or not, we here apply the method to reproduce some known  $s$ -wave Feshbach resonances. To show that our method is applicable to calculate higher partial-wave multichannel resonances, we calculate  $d$ -wave Feshbach resonance in the next section.

### 3.1. Two-channel model of $^{85}\text{Rb} + ^{85}\text{Rb}$ Feshbach resonance

Here we consider previously studied two-channel model [53] of Feshbach resonance in  $^{85}\text{Rb}$  atoms. According to the JILA experiment [54], the  $^{85}\text{Rb}$  condensate atoms were prepared in the hyperfine state ( $F = 2, m_F = -2$ ) which collide in open channel represented by reference potential  $V_{op}(r)$ . In the presence of an external magnetic field  $\mathbf{B}$ , the degeneracy of the hyperfine levels is lifted and the potentials associated with different asymptotic scattering channels are shifted with respect to each other. When the field-dependent energy  $E_{res}(\mathbf{B})$  of a closed channel vibrational state is tuned to the dissociation threshold of open channel, a near zero-energy scattering resonance occurs.

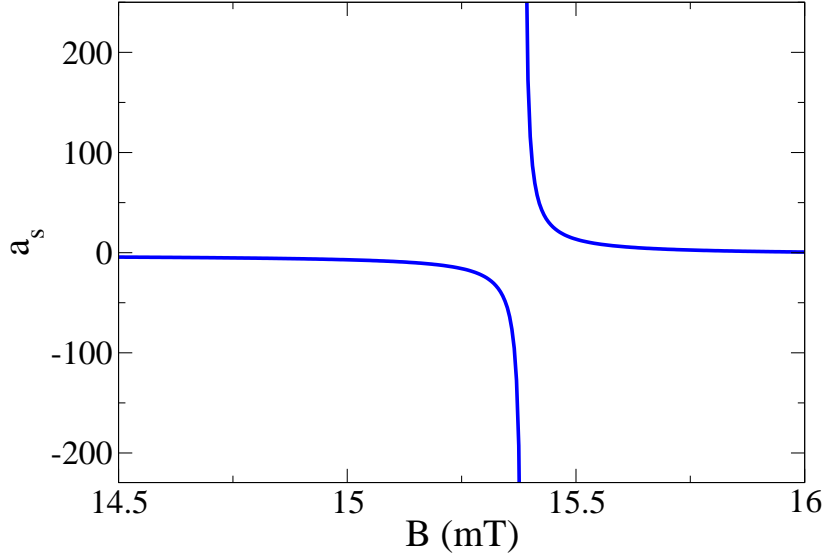


FIG. 1: The variation of the  $s$ -wave scattering length  $a_s$  of  $^{85}\text{Rb}$  as a function of magnetic field  $B$  in mT.

The Hamiltonian of the two-channel model can be expressed as

$$\hat{\mathbf{H}} = \begin{bmatrix} -\frac{\hbar^2}{2\mu} \frac{d^2}{dr^2} + V_{op}(r) & W(r) \\ W(r) & -\frac{\hbar^2}{2\mu} \frac{d^2}{dr^2} + V_{cl}(\mathbf{B}, r) \end{bmatrix}$$

where  $\mu$  is the reduced mass of  $^{85}\text{Rb}$ . The explicit analytical form of  $V_{op}$  is approximated by Lennard-Jones potential of the form

$$V_{op}(r) = 4\xi \left[ (\sigma/r)^{12} - (\sigma/r)^6 \right] \quad (22)$$

where  $\sigma = 10.075 a_0$  and  $4\xi\sigma^6 = C_6 = 4700 a_0$ . The background scattering length is  $a_{op} = -450 a_0$  for the open channel potential  $V_{op}$ . The potentials in both the channels have the same form but with the closed channel potential shifted upwards in energy, such that its threshold is at  $E_{th} + \Delta\mu B$ , where  $\Delta\mu$  represents the difference in magnetic moment between separated atoms and the bare resonance state. Therefore, the closed channel potential is given by

$$V_{cl}(r, B) = V_{op}(r) + E_{th} + \Delta\mu B \quad (23)$$

The closed channel potential is modeled as  $V_{cl} = V_{op} + E_{cl}(\mathbf{B})$  where  $E_{cl}$  follows the dependence of energy difference of the corresponding Zeeman hyperfine levels with the magnetic field as  $\hbar^{-1} \delta E_{cl} / \delta \mathbf{B} = -33.345 \text{ MHz/mT}$ . The coupling between the said two-channels is given by

$$W(r) = \beta \exp(-r/\alpha) \quad (24)$$

where  $\beta = 0.203 \text{ a.u.}$  and  $\alpha = 1 a_0$ . So, it is a five parameter model that characterizes the Feshbach resonance of  $^{85}\text{Rb}$ . Following the method as discussed in the section 2.1 and appendix A, we calculate the hyperbolic functions  $s_{c_i}$  and  $c_{c_i}$  related to the closed channel and sinusoidal functions  $s_{o_i}$  and  $c_{o_i}$  related to open channel. In order to calculate these functions numerically, we perform inward propagation from  $r = 100 a_0$  and  $r = 2000 a_0$  for closed and open channels, respectively. We carry out outward propagation in matrix form from  $r = 8 a_0$  to a certain distance  $r_m$ . We match the outward and inward solutions by a two-point matching procedure in spirit of QDT,  $\Phi = (\mathbf{s} + \mathbf{c}\mathbf{R})\mathbf{A}$ . where  $\mathbf{s}$ ,  $\mathbf{c}$  are diagonal matrices and  $\mathbf{A}$  is normalization constant. After matching those solutions, we get short range  $\mathbf{R}$  matrix and the matrix  $\mathbf{A}$ . The matching point is chosen at a separation where the function  $\phi_i(r)$  crosses the first anti-node from outer side and it appears near  $40 a_0$  for this two channel model system. In this regime, magnitude of the off-diagonal potential is negligible compared to the diagonal potential. For a two-channel model,  $\mathbf{R}$  matrix is simply a number  $R$  and the phase shift ( $\delta$ ) is related to  $R$  by  $\tan \delta(k) = R$  and the scattering length  $a_s = -\lim_{k \rightarrow 0} \tan \delta(k)/k$ .

In figure.1, we show the variation of  $a_s$  as a function of magnetic field  $B$ . This figure clearly demonstrates resonance near the magnetic field 15.4 mT. The experimentally observed Feshbach resonance of  $^{85}\text{Rb}$  was reported at 15.5 mT [55]. So, our result is very close to the experimental value. In figure.2, we plot the square of absolute value of  $T$ -matrix as a function of energy

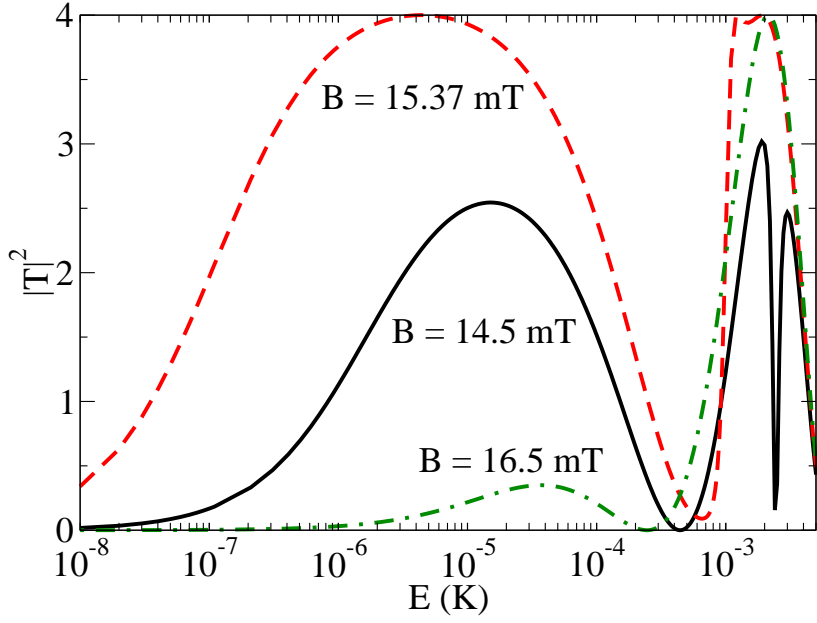


FIG. 2: The variation of the absolute value of the square of T-matrix elements as a function of energy  $E$  in Kelvin of  $^{85}\text{Rb}$  for three different values of magnetic field.

in kelvin for the different values of  $B$ . Near magnetic field  $B = 15.4$  mT i.e near the resonance, the value of  $|T|^2$  approaches its maximum value of 4 implying that the phase shift goes through  $\pm\pi/2$  and thus establishing the occurrence of FR.

Before we end this subsection, we wish to comment on the validity of the neglect of the off-diagonal inter-channel coupling matrix elements  $W_{ij}(r)$  ( $i = 1, 2$  but  $i \neq j$ ) for  $r > r_m$ . The question naturally arises to what extent the residual matrix  $W^{res}(r)$  where  $W_{ii}^{res} = 0$  and  $W_{ij}^{res} = 0$  ( $i \neq j$ ) for  $r \leq r_m$  and  $W_{ij}^{res} = W_{ij}(r)$  ( $i \neq j$ ) for  $r > r_m$  can affect the results through final-state interactions. To test this validity, we define the ratio  $\lambda = 2W_{12}(r_m)/(W_{11}(r_m) + W_{22}(r_m))$  of off-diagonal element  $W_{12}$  to the average  $(W_{11} + W_{22})/2$  of the two diagonal elements at  $r = r_m$ . If  $\lambda \ll 1$  then one can justify that the inter-channel coupling is indeed negligible for  $r > r_m$ . For the two-channel problem discussed above, the value of  $\lambda$  is smaller than unity by several orders.

### 3.2. $s$ -wave Feshbach resonance of $^6\text{Li}$

In this sub-section we reproduce a known FR of fermionic  $^6\text{Li}$  atoms by our all numerical MQDT method. We consider 5 asymptotic channels to reproduce the broad Feshbach resonance near 832 G. The Hamiltonian can be written in the form

$$H = T(r) + \sum H^{int} + V^c \quad (25)$$

where  $T(r)$  is the kinetic energy term,  $V^c$  is the interatomic potential on electronic spin state  $\vec{S}_1$  and  $\vec{S}_2$  of the two atoms. The interaction may be written in the form of

$$V^c = V_0(r)P_0 + V_1(r)P_1 \quad (26)$$

where  $P_0 = 1/4 - S_1 \cdot S_2$  and  $P_1 = 3/4 + S_1 \cdot S_2$  are the projection operators for two-electron singlet and triplet states, respectively; and  $V_0(r)$  and  $V_1(r)$  are the singlet and triplet potentials, respectively. This interaction is therefore diagonal in molecular or adiabatic basis  $|IM_J; SM_S\rangle$ , so that

$$\langle S'M'_S; I'M'_I | V^c | SM_S; IM_I \rangle = \delta_{I,I'} \delta_{M_I M'_I} \delta_{S,S'} \delta_{M_S M'_S} V_S \quad (27)$$

where  $\vec{S} = \vec{s}_1 + \vec{s}_2$  and  $\vec{I} = \vec{i}_1 + \vec{i}_2$ ,  $\vec{s}_1$  and  $\vec{s}_2$  being the electronic spins and  $\vec{i}_1$  and  $\vec{i}_2$  being nuclear spins of the two atoms. The interaction Hamiltonian  $\sum H^{int}$  can be written as

$$H^{int} = H_{hf} + H_B \quad (28)$$

where,  $H_{hf}$  and  $H_B$  represent hyperfine and Zeeman interactions, respectively.

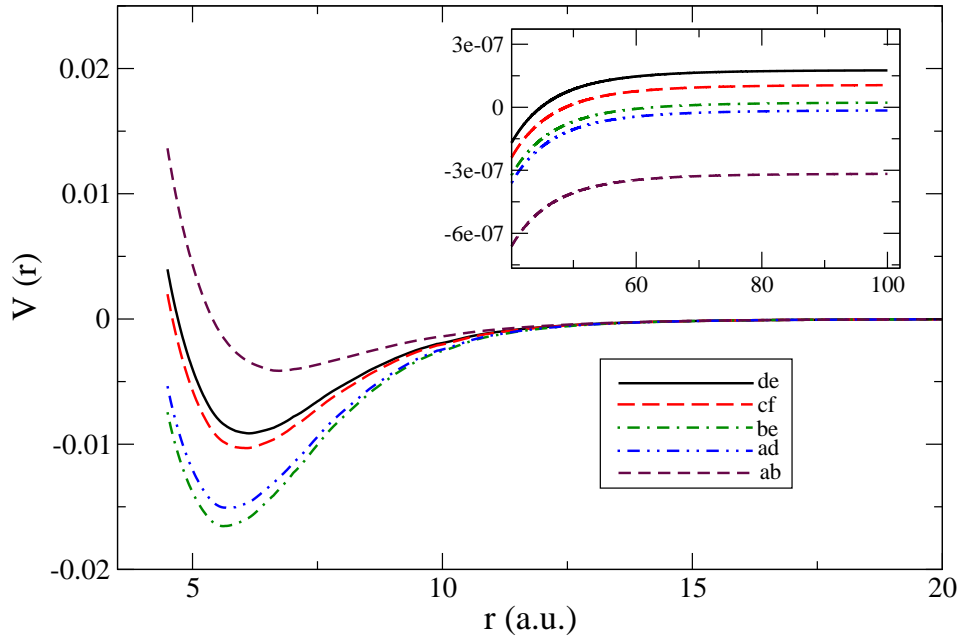


FIG. 3: The variations of five diagonal potentials of  ${}^6\text{Li}$  system as a function of internuclear distance  $r$  at short range regime for the magnetic field  $B = 832.1$  G. The corresponding asymptotes are shown in the inset of the figure.

Now, when the two atoms are well separated, the non-interacting atoms can be treated individually in terms of atomic basis  $|f_j m_j\rangle$  for atom  $j$ , where  $\vec{f}_j = \vec{s}_j + \vec{i}_j$  and  $m_j$  is the projection of total spin for a single atom. The hyperfine interaction for single atom can be written as

$$H_{hf} = \frac{a_{hf}}{\hbar^2} \vec{s}_j \cdot \vec{i}_j = \frac{a_{hf}}{2\hbar^2} (\vec{f}_j^2 - \vec{s}_j^2 - \vec{i}_j^2) = \frac{a_{hf}}{2\hbar^2} [f(f+1) - s(s+1) - i(i+1)] \quad (29)$$

and  $a_{hf}$  is the hyperfine constant.

Hence, for two colliding atoms at large separation, the suitable representation would be uncoupled hyperfine basis  $|f_1 m_1, f_2 m_2\rangle$ . So in the absence of magnetic field, interaction Hamiltonian can be written as  $\sum H^{int} = H_{hf} = H_1^{hf} + H_2^{hf}$ . The atomic or diabatic or long-range basis can also be expressed in coupled hyperfine representation  $| (f_1 f_2) F m_F \rangle$  and the hyperfine interaction is diagonal in this basis. Here,  $F = f_1 + f_2$  is total hyperfine spin, and  $m_F$  is the projection of total hyperfine spin. Now, we have to convert the central potential in the diabatic basis,  $| (f_1 f_2) F m_F \rangle$ .

$$\langle (f_1 f_2) f m_f | V^c | (f'_1 f'_2) f' m'_f \rangle = \sum_{S, I, M_S, M_I} V_S \langle (f_1 f_2) f m_f; l m_l | S M_S; I M_I; l' m'_l \rangle \langle S M_S; I M_I; l' m'_l | (f_1 f_2) f m_f; l m_l \rangle \quad (30)$$

The transformation of the diabatic basis (coupled hyperfine representations) to the adiabatic basis (short range representations) is as follows

$$\langle S M_S; I M_I; l' m'_l | (f_1 f_2) f m_f; l m_l \rangle = \delta_{l'l} \delta(m_l m'_l) \langle S M_S; I M_I | f m_f \rangle \sqrt{(2f_1+1)(2f_2+1)(2S+1)(2I+1)} \begin{Bmatrix} s_1 & i_1 & f_1 \\ s_2 & i_2 & f_2 \\ S & I & f \end{Bmatrix} \left( \frac{1 + (1 - \delta_{f_1 f_2})(-1)^{S+I+l}}{\sqrt{2 - \delta_{f_1 f_2}}} \right) \quad (31)$$

Here,  $\langle S M_S; I M_I | f m_f \rangle$  is Clebsch Gordon coefficient and the quantity in curly bracket is known as  $9j$ -symbol. Here  $m_1 + m_2 = m_f = m'_1 + m'_2 = M_S + M_I$ . If the magnetic field is sufficiently weak, then as a first approximation one can use these channel states. However, when the magnetic field is strong enough, the asymptotic Hamiltonian is no longer diagonal due to presence of Zeemann terms. A new basis denoted by  $| \tilde{f} \tilde{m}_f \rangle$ , which is suitable for scattering in the presence of a magnetic field is obtained by diagonalizing asymptotic form of the Hamiltonian. But, in this new basis, central potential  $V^c$  can not be diagonalized and the resulting off-diagonal terms will provide the coupling which may eventually lead to multichannel resonances. Let

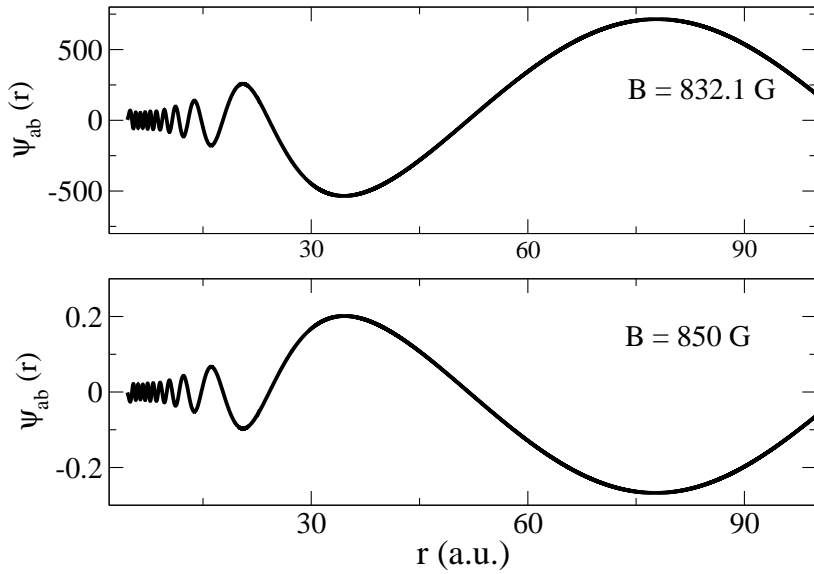


FIG. 4: Energy-normalized wave functions for the open channel (ab) of  ${}^6\text{Li}$  as a function of internuclear separation  $r$  for two different values of magnetic fields.

TABLE I: Separated five atomic channels for the  $s$ -wave Feshbach resonance of  ${}^6\text{Li}$ . The projection of total angular momentum  $M_F = 0$ .

channels	$(f_1, f_2)$	$(m_{f_1}, m_{f_2})$
ab	$(\frac{1}{2}, \frac{1}{2})$	$(+\frac{1}{2}, -\frac{1}{2})$
ad	$(\frac{1}{2}, \frac{3}{2})$	$(+\frac{1}{2}, -\frac{1}{2})$
be	$(\frac{1}{2}, \frac{3}{2})$	$(-\frac{1}{2}, +\frac{1}{2})$
cf	$(\frac{3}{2}, \frac{3}{2})$	$(-\frac{3}{2}, +\frac{3}{2})$
de	$(\frac{3}{2}, \frac{3}{2})$	$(+\frac{1}{2}, -\frac{1}{2})$

$|a\rangle = |SM_S; IM_I\rangle$  denote adiabatic basis that diagonalize  $V^c$ ;  $|b\rangle = |f_1 m_1; f_2 m_2\rangle$  is asymptotic basis that diagonalizes  $H_{hf}$  and  $|\tilde{b}\rangle = |\tilde{f} \tilde{m}_f\rangle$  diagonalises  $H_{hf} + H_B$ , respectively. So, we need to express the whole problem in  $|\tilde{b}\rangle$  basis which is physically relevant basis for our purpose at  $r \rightarrow \infty$ . We consider the following steps in order to obtain the diagonal and off-diagonal potentials in the physically relevant basis. In first step, we express  $(H_{hf} + H_B)$  in  $|b\rangle$  basis, these can be done analytically and leads to a non-diagonal matrix. Then, this matrix is numerically diagonalised to obtain eigenvalues which define the threshold energy of the channel and the eigenvectors for transformations from  $|b\rangle$  to  $|\tilde{b}\rangle$  basis.

$$|\tilde{b}_j\rangle = \sum_i |b_i\rangle \langle b_i | \tilde{b}_j\rangle = \sum_i c_{ji} |b_j\rangle \quad (32)$$

In the next step,  $V^c$  is transformed from  $|a\rangle$  basis to  $|b\rangle$  basis which leads to off-diagonal terms. Finally,  $V^c$  is transformed from  $|b\rangle$  basis to  $|\tilde{b}\rangle$  basis using  $c_{ji}$  coefficients. During the transformations, the projection of the total angular momentum  $M_F = m_{f_1} + m_{f_2}$  is conserved. The quantization axis is chosen to be along the direction of the magnetic field.

${}^6\text{Li}$  has nuclear and electronic spin  $i = 1$  and  $= 1/2$ , respectively. Here we take five channels to describe  $s$ -wave Feshbach resonance near 832 G following the work by Chin *et al* [3]. These five channels are listed in Table.I. In figure.3, we plot five diagonal potentials in short range regime as a function of  $r$  for a particular value of magnetic field  $B = 832.1$  G. In the inset of the figure, we show the asymptotic long range part of the potentials for the chosen five channels. The energy of the said channels increases from ‘ab’ to ‘de’ as a function of  $B$  [3]. The channel ‘ab’ is open and the other four channels are closed. For the open channel, we consider inward propagation from asymptotic region  $r = 2000 a_0$  and for closed channels we start propagation from  $r = 150 a_0$ . For this system, the matching point is chosen at  $r_m \sim 22 a_0$ .

In figure.4, we plot the wave functions for open channel in upper and lower panels for magnetic field  $B = 832.1$  G and  $B = 850$  G, respectively. From this figure we notice that the amplitude of the wave function is much higher at  $B = 832.1$  G than  $B = 850$  indicating an effect of the resonance near 832.1 G. In figure.5 we show  $|T|^2$  as a function of energy for the said two values of magnetic fields. For the field  $B = 850$  G, there is hardly any effect of resonance unlike that for  $B = 832.1$  G at which Feshbach resonance occurs as energy decreases below 1 microKelvin.

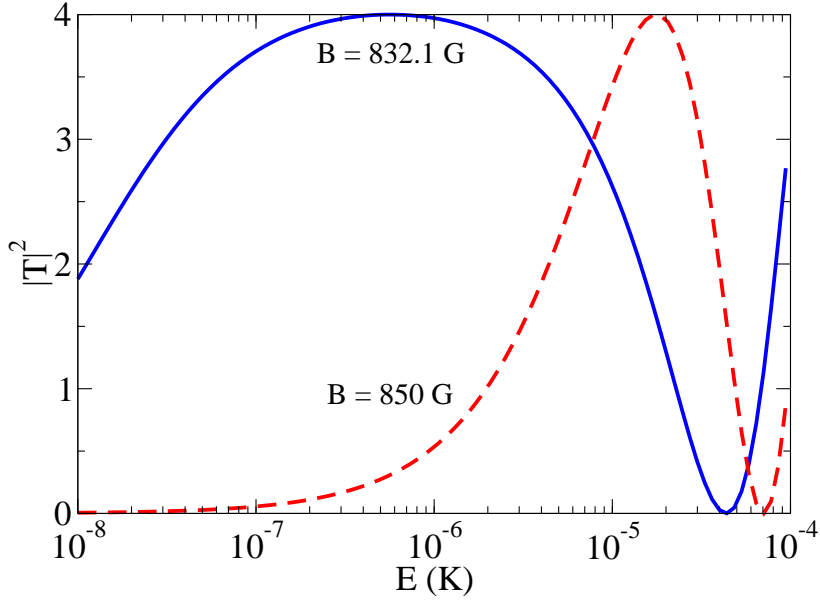


FIG. 5: The variation of  $|T|^2$  as a function of  $E$  in Kelvin for two different values of  $B = 832.1$  G (blue, solid) and  $B = 850$  G (red, dashed).

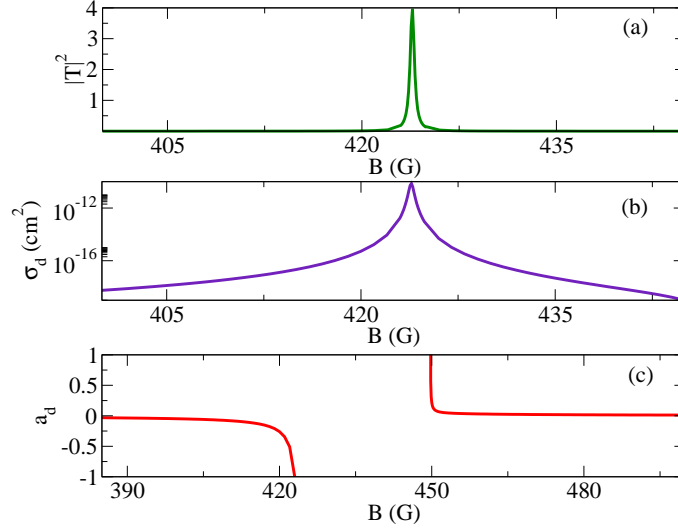


FIG. 6: Shown are the  $|T|^2$ ,  $\sigma_d$  and the dimensionless  $d$ -wave scattering length  $a_d$  of  $^{87}\text{Rb} + ^{85}\text{Rb}$  as a function of  $B$  in the panels (a), (b) and (c), respectively.

In passing, we verify whether we can really neglect the off-diagonal potential terms for  $r > r_m$ . For this we evaluate the  $\lambda$  parameter as defined in the preceding subsection for the lowest two channels, that is, the lowest open channel and the lowest closed channel. We find  $\lambda \simeq 0.01$ . So, we can reasonably neglect the off-diagonal terms for  $r > r_m$ .

#### 4. $d$ -WAVE FESHBACH RESONANCE OF $^{87}\text{RB} + ^{85}\text{RB}$ SYSTEM

For higher partial-wave ( $\ell > 0$ ) scattering in the presence of an external magnetic field,  $m_F$  no longer remains good quantum number, but only the projection  $M_J$  on the quantization axis of the total angular momentum  $\mathbf{J} = \mathbf{f} + \vec{\ell}$  is conserved. The asymptotic or uncoupled basis  $|f_1 m_1, f_2 m_2; \ell m_\ell\rangle$  can be expressed in terms of the coupled basis in the following way

$$|f_1 m_1, f_2 m_2; \ell m_\ell\rangle = \sum_f \langle f m_f | f_1 m_1, f_2 m_2\rangle |f m_f\rangle | \ell m_\ell\rangle. \quad (33)$$

The matrix element of the central potential is given by

$$\begin{aligned} \langle f_1 m_1, f_2 m_2; \ell m_\ell | V^c | f'_1 m'_1, f'_2 m'_2; \ell' m'_\ell \rangle &= \delta_{\ell \ell'} \delta_{m_\ell m'_\ell} \sum_{f, f'} \langle f' m'_f | f'_1 m'_1, f'_2 m'_2 \rangle \langle f_1 m_1, f_2 m_2 | f m_f \rangle \\ &\times \sum_{S, I, M_S, M_I} V_S \langle (f_1 f_2) f m_f | SM_S, IM_I \rangle \langle SM_S, IM_I | (f'_1 f'_2) f' m'_f \rangle \end{aligned} \quad (34)$$

where  $\mathbf{f}_1 + \mathbf{f}_2 = \mathbf{f}$ ,  $\mathbf{f}'_1 + \mathbf{f}'_2 = \mathbf{f}'$ ,  $m_1 + m_2 = m_f$  and  $m'_1 + m'_2 = m'_f$ . Here

$$\begin{aligned} \langle SM_S, IM_I | (f_1 f_2) f m_f \rangle &= \langle SM_S, IM_I | f m_f \rangle \\ &\frac{1}{\sqrt{(2f_1 + 1)(2f_2 + 1)(2S + 1)(2I + 1)}} \\ &\left\{ \begin{array}{ccc} s_1 & i_1 & f_1 \\ s_2 & i_2 & f_2 \\ S & I & f \end{array} \right\} \left( \frac{1 + (1 - \delta_{f_1 f_2})(-1)^{S+I+l}}{\sqrt{2 - \delta_{f_1 f_2}}} \right) \end{aligned} \quad (35)$$

where  $\langle SM_S; IM_I | f m_f \rangle$  is Clebsch Gordon coefficient and the quantity in curly bracket is known as  $9j$ -symbol. Here  $m_1 + m_2 = m_f = m'_1 + m'_2 = M_S + M_I$ .

From the effective-range expansion, the generalized scattering length for  $l$ -th partial wave can be expressed as  $a_l = -\tan \delta_l / k^{2l+1}$  in the limit  $E \rightarrow 0$ . For  $s$ - and  $p$ -wave, the quantity  $a_{l=0}$  and  $a_{l=1}$  correspond to the scattering length and scattering volume, respectively. We define the dimensionless  $d$ -wave scattering length  $a_d = a_l / \beta$ , where  $\beta = (2\mu C_6 / \hbar^2)^{1/4}$  is the characteristic length scale.

From the above consideration, we wish to calculate the  $d$ -wave FR in an ultracold mixture of  $^{87}\text{Rb}$  and  $^{85}\text{Rb}$  atoms as recently studied experimentally by You's group [49]. The  $d$ -wave FR may arise from two different mechanistic pathways. In the first pathway the FR occurs mainly due to the coupling between an  $l = 0$  ( $l = 2$ ) open channel and an  $l' = 2$  ( $l' = 0$ ) closed channel, fulfilling the selection rule  $\Delta l = 2$ . In the second pathway, the  $d$ -wave FR occurs for  $\Delta l = 0$  for which there is a direct coupling of an open channel having  $l = 2$  with several other closed channels with  $l' = 2$ . Experimentally, the atoms are initially prepared in the hyperfine channel  $^{87}\text{Rb} | f = 1, m_f = -1 \rangle + ^{85}\text{Rb} | f = 2, m_f = -2 \rangle$  [49]. For  $^{85}\text{Rb}$ , nuclear spin  $i_1 = 5/2$  and for  $^{87}\text{Rb}$ ,  $i_2 = 3/2$ . If we neglect the second order spin-spin interaction, then the channels that correspond to different  $m_f$  and  $M_J = M_F + m_f$  but same  $M_F = m_{f_1} + m_{f_2}$  are degenerate. For our numerical computation, we consider only one open channel with  $f_{85} = 2$ ,  $m_{f_{85}} = -2$ ,  $f_{87} = 1$ ,  $m_{f_{87}} = -1$ ,  $\ell = 2$ , that is, the channel in which the atoms are initially prepared. We consider several closed channels. We have found that a 6-channel calculation with one open and five closed channels yield good results. These chosen channels are enlisted in table.II with (1)-(5) being closed channels and (6) the open channel.

TABLE II: Six asymptotic channels for the  $d$ -wave Feshbach resonance of  $^{87}\text{Rb}$  and  $^{85}\text{Rb}$ .  $f_1$  and  $f_2$  represent the hyperfine quantum numbers of atoms  $^{87}\text{Rb}$  and  $^{85}\text{Rb}$ , respectively.

channels	$(f_1, f_2)$	$(m_{f_1}, m_{f_2})$
1	(2, 3)	(-2, -1)
2	(2, 3)	(-1, -2)
3	(1, 3)	(-1, -2)
4	(2, 2)	(-2, -1)
5	(1, 3)	(0, -3)
6	(1, 2)	(-1, -2)

For the open channel we start inward propagation from a large separation ( $r \geq 1000a_0$ ) with asymptotic solution

$$\hat{J}_2 \simeq \left( \frac{3}{z^2} - 1 \right) \sin z - \frac{3}{z} \cos z \quad (36)$$

where  $z = kr$ . We calculate the irregular solution by solving the Wronskian equation. The irregular solution asymptotically behaves like

$$\hat{n}_2 \simeq \frac{3}{z} \sin z + \left( \frac{3}{z^2} - 1 \right) \cos z \quad (37)$$

For closed channels, we choose our starting point for inward propagation nearly at  $r \simeq 140 a_0$ . We perform outward propagation from  $r = 9.46a_0$  to  $r_m$  in  $6 \times 6$  matrix form and match with numerically calculated quantum defect function using two-point matching procedure. Our matching point lies nearly at  $r_m = 40 a_0$ .

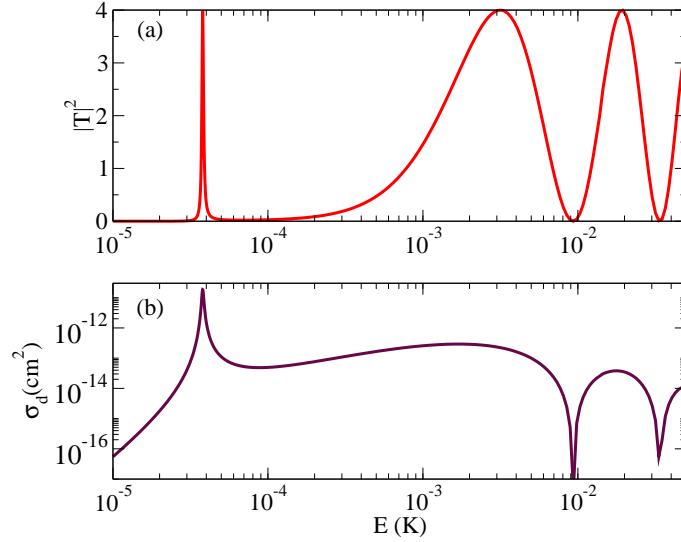


FIG. 7: The variation of  $|\mathbf{T}|^2$  and  $\sigma_d$  as a function of  $E$  in the panels (a) and (b), respectively.

Next, to study the effects second order spin-spin interaction on the resonance, we calculate the multi-channel spin-spin interactions terms and include them in our all numerical MQDT calculations. The Hamiltonian for the spin-spin interaction can be expressed as

$$H_{ss} = -\frac{\alpha^2}{\sqrt{6}R^3} \sum_{q=-2}^2 (-1)^q \hat{C}_q^{(2)} \Sigma_{-q}^{(2)} \quad (38)$$

where  $\alpha$  is the fine structure constant,  $\hat{C}_q^{(2)}$  is the reduced spherical harmonics and  $\Sigma_{-q}^{(2)} = (s_1 \otimes s_2)_{-q}^{(2)}$  is a second order tensor formed from the spin operators. The spin-spin matrix element between two basis states  $|\tilde{b}_j\rangle$  and  $|\tilde{b}_{j'}\rangle$  is given by

$$\langle \tilde{b}_{j'} | H_{ss} | \tilde{b}_j \rangle = \sum_{i i'} c_{j' i'}^* c_{j i} \langle b_{i'} | H_{ss} | b_i \rangle \quad (39)$$

Considering  $|b_i\rangle \equiv |f_1 m_1, f_2 m_2; \ell m_\ell\rangle$  and  $|b_{i'}\rangle \equiv |f'_1 m'_1, f'_2 m'_2; \ell' m_{\ell'}\rangle$ , we have

$$\begin{aligned} \langle b_{i'} | H_{ss} | b_i \rangle &= \sum_{f, f'} \sum_{I, M_I} [\langle f m_f | f_1 m_1, f_2 m_2 \rangle] \times [\langle SM_S, IM_I | (f_1 f_2) f m_f \rangle] \\ &\times [\langle f'_1 m'_1, f'_2 m'_2 | f' m'_f \rangle] \times [\langle (f'_1 f'_2) f' m'_f | SM'_S, IM_I \rangle] \\ &\times \left[ -\frac{\alpha^2}{\sqrt{6}R^3} \right] \sum_{q=-2}^2 (-1)^q \langle \ell' m_{\ell'} | \hat{C}_q^{(2)} | \ell m_\ell \rangle \times \langle SM'_S | \Sigma_{-q}^{(2)} | SM_S \rangle \end{aligned} \quad (40)$$

Here  $M_S = m_f + m_\ell - m_I$  and  $M'_S = m_{f'} + m_{\ell'} - m'_I$ . Only for the triplet state ( $S = 1$ ) the matrix element is nonzero. This given the selection rules  $\Delta\ell = 0, \pm 2$  and also fulfill the criteria:  $m_{\ell'} = m_\ell + q$  and  $M'_S = M_S - q$ . In our calculation, we incorporate the spin-spin interaction in matrix form up to matching point  $r_m$  and beyond  $r_m$  the  $H_{ss}$  is included in the diagonal channels only.

## 5. RESULTS AND DISCUSSIONS

We first present results of our 6-channel calculations of  $d$ -wave FR without taking spin-spin interaction into account in Figs. 6 and 7; and then show the effects of spin-spin interactions on the FR in Fig. 8. Figure 6 displays  $|\mathbf{T}|^2$ ,  $d$ -wave scattering cross section  $\sigma_d$  and the dimensionless  $d$ -wave scattering length  $a_d$  as a function of  $B$  for fixed energy  $E = 37 \mu\text{K}$ . Figure 6(a) shows that the quantity  $|\mathbf{T}|^2$  takes its maximum value 4 near the magnetic field 424.1 G indicating that the scattering phase shift goes through  $\pm\pi/2$  near this magnetic field. This feature is a clear signature of a scattering resonance. Figure 6(b) shows the resonant variation of  $\sigma_d$  in  $\text{cm}^2$  while Fig. 6(c) exhibits divergence behavior of  $a_d$  near  $B = 424.1$  G illustrating further the existence of the  $d$ -wave FR. We also plot  $|\mathbf{T}|^2$  as a function of energy in the panel (a) of Fig. 7 at the magnetic field 424.1 G. We notice that the quantity  $|\mathbf{T}|^2$  attains its maximum value 4 near the energy  $37 \mu\text{K}$ . The panel (b) of Fig. 7 shows the resonance in the variation of  $\sigma_d$  as a function of  $E$ .

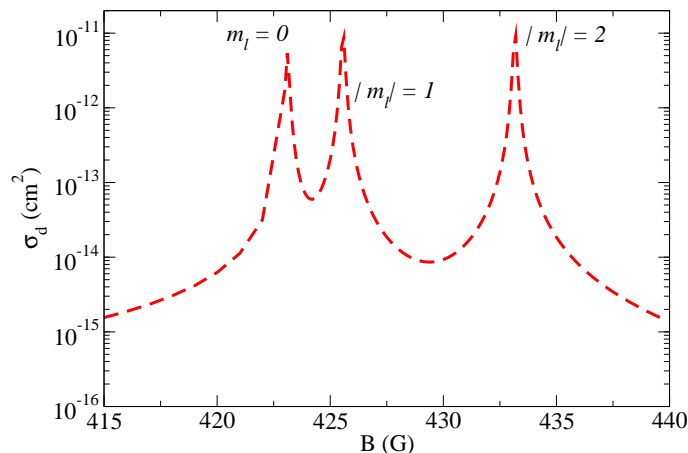


FIG. 8: The variation of the  $\sigma_d$  as a function of  $B$  illustrates the triplet structure of the  $d$ -wave Feshbach resonance.

In our numerical calculations, the data for the ground-state singlet and triplet potentials of  $\text{Rb}_2$  are taken from Ref. [56]. The value of vdW coefficient reported in Ref. [56] is  $C_6 = 4719$  a.u. However, its experimental value is not precisely known. Therefore, one can optimize it in order to obtain a good agreement between numerical results and experimental observations [57]. We find that if we slightly change it to  $C_6 = 4740$  a.u, we get a better agreement with the experimental results.

Experimentally, a broad single-peak  $d$ -wave Feshbach resonance corresponding to the incident channel  $^{87}\text{Rb}|f=1, m_f=-1\rangle + ^{85}\text{Rb}|f=2, m_f=-2\rangle$  was detected at 423 G at a temperature of  $16 \mu\text{K}$ . Two-channel quantum defect calculations that make use of analytical solutions of van der Waal's potential [43, 44] predicts this broad resonance at 440.9 G [49]. Our 6-channel calculations yield resonance at 424.1 G which is much closer to the experimentally found resonant field value. Experimentally, it was further observed that on lowering the temperature to  $1.2 \mu\text{K}$ , the single broad peak had been split into two peaks. On further lowering of the temperature to  $0.4 \mu\text{K}$ , a three-peak structure appears.

In figure 8 we show the effect of the spin-spin interaction on  $\sigma_d$  as a function of  $B$ . The effect is manifested at a lower energy  $E = 25 \mu\text{K}$  in the form of a three-peak structure in the resonance near 424.1 G. The left peak is due to the  $m_l = 0$ , while the middle and the right peaks account for the  $|m_l| = 1$  and  $|m_l| = 2$ , respectively. Although, experimentally the triplet structure in the resonance appeared at a temperature of  $0.4 \mu\text{K}$ , we find such triplet structure at  $E = 25 \mu\text{K}$  which is lower than that at which the single-peak resonance without spin-spin couplings appears. Our results qualitatively agree well with the experimental ones in that the spin-spin interactions lead to the shifts of the resonance point towards higher magnetic fields and the widths of the three peaks are quite narrow ( $\simeq 0.1$  G). Perhaps, thermal broadening at a higher temperature washes out the triplet structure leading to a broad single-peak resonance. Since the widths of the three peak structures are quite narrow, the resolution of the triplet structure will be possible if the temperature is smaller than the average width (in unit of energy) of the peak structures.

## 6. CONCLUSIONS

We have developed an MQDT in a complete numerical approach using standard Numerov-Cooley algorithm and the numerical solution of the Wronskian equation. One of the primary base functions  $\phi_i(r)$  is calculated by single-channel inward propagation from asymptotic region to short range. The other base function is calculated by numerically solving the Wronskian equation. In our method, we select a matching point  $r_m$  near a separation where first anti-node of function  $\phi_i(r)$  for a closed channel  $i$  appears as it propagates inward, and so it lies in classically allowed region. After making inward propagation, an outward propagation is carried out in matrix form. During the propagation, linear independence is maintained throughout short as well as long range regime. In our method, linear independence is automatically maintained since outward multichannel propagation is carried out only within the classically allowed region. Linear independence becomes a particular issue of concern when multichannel wave function or matrix wave function is propagated through classically forbidden region. We have applied our method in three cases: (i) a standard two-channel model calculation is used for describing the  $s$ -wave Feshbach resonance of  $^{85}\text{Rb}$  atoms, (ii) a five-channel calculation is performed to describe the  $s$ -wave magnetic Feshbach resonance of fermionic  $^6\text{Li}$  system near the magnetic field  $B = 832.1$  G. and (iii) a six-channel calculation is carried out to calculate the  $d$ -wave FR of  $^{85}\text{Rb}$ - $^{87}\text{Rb}$  system near the magnetic field 424.1 G. While the first two cases are considered only to standardize our method, new results are obtained in the third case. Our results on  $d$ -wave FR reasonably agree well with the experimental observations as reported in [49] a few years ago.

We have justified the neglect of inter-channel couplings for  $r > r_m$  by verifying whether the  $\lambda$ -parameter is sufficiently small. Suppose,  $\lambda$  is smaller than unity but not too small to neglect. In that case, the effects of the residual potential element  $W_{ij}^{res}$  for  $r > r_m$  can readily be taken into account perturbatively by constructing real space Green function using the numerical reference

functions. Since our numerical reference functions are calculated taking into account all the long-range potential terms, the Green function so calculated will be more accurate. Thus, using our method one can easily obtain complete information of wave function throughout the entire range for both open or closed channels. As in chemical process like PA, the information of Franck Condon factor which is associated with wave function of scattering continuum plays an important role. Therefore, all continuum-bound spectroscopy involving atom-atom [11] or atom-ion systems [58–60] can be explained by our MQDT technique. Our method is numerically more precise but easy to implement, and so can be applied to all sorts of realistic long-range potentials. A complete information on multi-channel wave function or density matrix is crucially important for exploring aspects of quantum information or quantum gate operation by controlled collisions of cold atoms [61, 62].

### Acknowledgments

One of us (Dibyendu Sardar) is thankful to CSIR Government of India for a financial support.

### Appendix A: Numerical method of solving Wronskian equation

Let us consider, the two linearly independent (LI) solutions  $\psi_i(r)$  and  $\phi_i(r)$  of the following linear second order homogeneous differential equation

$$y''(r) + Q(r)y(r) = 0 \quad (\text{A1})$$

Hence,

$$\psi_i''(r) + Q(r)\psi_i(r) = 0 \quad (\text{A2})$$

$$\phi_i''(r) + Q(r)\phi_i(r) = 0 \quad (\text{A3})$$

Multiplying Eq.A2 by  $\phi_i$ , Eq.A3 by  $\psi_i$  and subtracting the resulting equations from each other, we get  $W'(r) = 0$  where  $W(r) = W[\phi_i, \psi_i] = \phi_i'(r)\psi_i(r) - \psi_i'(r)\phi_i(r)$  is the Wronskian between  $\phi_i(r)$  and  $\psi_i(r)$ , implying

$$\phi_i'(r)\psi_i(r) - \psi_i'(r)\phi_i(r) = C \quad (\text{A4})$$

where  $C$  is a constant.

Let us first consider two LI functions for a closed channel  $i$ . Suppose, the function  $\phi_i(r)$  has the asymptotic boundary condition  $\phi_i \sim \exp(-\kappa_i r)$ . We numerically calculate this function by inward integration of single-channel Schrödinger equation using this boundary condition. So, the other LI function  $\psi_i(r)$  must satisfy the boundary condition  $\psi_i(r) \sim \exp(\kappa r)$  as  $r \rightarrow \infty$ . Therefore, we set  $C = -2\kappa_i$  for a closed channel. Now, the problem at hand is to solve the Eq. (A4) for the second LI solution  $\psi(r)$ .

Let  $r_a$  be a point in this large  $r$  regime, and the value of the first solution ( $\phi_i$ , say) be known at  $r_a - h$ ,  $r_a$  and  $r_a + h$ , with  $h$  being the step size for propagation. Then  $\phi_i'(r_a)$  can be calculated as

$$\phi_i'(r_a) = \frac{\phi_i(r_a + h) - \phi_i(r_a - h)}{2h} \quad (\text{A5})$$

and the value of the second solution at  $r_a$  is

$$\psi_i(r_a) = \exp(\kappa r_a) \quad (\text{A6})$$

From the Wronskian Eq. (A4), we can write

$$\psi_i'(r_a) = \frac{-2\kappa + \psi_i(r_a)\phi_i'(r_a)}{\phi_i(r_a)} \quad (\text{A7})$$

The value of the second derivative  $\psi_i''(r_a)$  is given by the Schroedinger Eq.A1 itself as

$$\psi_i''(r_a) = -Q(r_a)\psi_i(r_a) \quad (\text{A8})$$

Now, a Taylor's series expansion of  $\psi$  about  $r_a$  gives

$$\psi_i(r_a - h) = \psi_i(r_a) - h\psi_i'(r_a) + \frac{h^2}{2}\psi_i''(r_a) \quad (\text{A9})$$

Knowing the value of  $\psi_i(r_a)$ ,  $\psi'_i(r_a)$  and  $\psi''_i(r_a)$  from Eq.A6, Eq.A7 and Eq.A8 respectively, we can get  $\psi_i(r_a - h)$  from Eq.A9. We repeat over and over the steps Eq.A5-Eq.A9 and calculate  $\psi_i$  in the desired range. While executing the propagation, we avoid dealing with a too small or a too large number by setting the asymptotic boundary function  $\phi_i(r) = \mathcal{N} \exp(-\kappa r)$  with a judiciously chosen normalization factor  $\mathcal{N}$ . The integration of Wronskian equation for finding  $\psi_i(r)$  may be restricted over a limited region near the outer turning point in order to avoid the appearance of a large number. For finding  $\psi_i(r)$  by numerical integration of the Wronskian equation, it is not necessary that one should perform inward propagation starting from the asymptotic separation. One can instead carry out outward propagation starting from a node point of  $\phi_i(r)$  in the classically allowed region. In that case, the inward propagation for  $\phi_i(r)$  should be extended beyond the first node point counted from the outer side. However, the matching should be done at or near the first anti-node point.

After calculating numerical functions for closed channels, we calculate pair functions for open channels. For an open channel  $i$ , we set  $C = k_i$  and the asymptotic boundary condition

$$\phi(r) \sim \sin(k_i r - l\pi/2) \quad (\text{A10})$$

We calculate  $\phi(r)$  numerically by inward integration of the Schrödinger equation. We calculate the other LI solution  $\psi_r$  that asymptotically behaves as

$$\psi(r) \sim \cos(k_i r - l\pi/2) \quad (\text{A11})$$

by solving the Wronskian equation by the same procedure as in the case of the closed channel, but at the nodes of  $\phi(r)$  we set  $\psi(r) = C/\phi'(r)$ .

- 
- [1] N. Balakrishnan, J. Chem. Phys. **145**, 150901 (2016).  
[2] M. T. Bell and T. P. Softley, Mol. Phys. **107**, 99 (2008).  
[3] C. Chin, R. Grimm, P. Julienne and Tiesinga, Rev. Mod. Phys. **82**, 1225 (2010).  
[4] T Köhler, K. Góral, and P. S. Julienne, Rev. Mod. Phys. **78**, 1311 (2006).  
[5] S. Inouye, M. R. Andrews, J. Stenger, H. J. Miesner, D. M. Stamper-Kurn and W. Ketterle, Nature **392**, 151 (1998); J. L. Roberts, N. R. Claussen, J. P. Burke, C. H. Greene, E. A. Cornell, and C. E. Wieman, Phys. Rev. Lett. **81**, 5109 (1998); P. Courteille, R. S. Freeland, D. J. Heinzen, F. A. van Abeelen, and B. J. Verhaar, Phys. Rev. Lett. **81**, 69 (1998).  
[6] I. Bloch, J. Dalibard, and W. Zwerger, Rev. Mod. Phys. **80**, 885 (2008); S. Giorgini, L. P. Pitaevskii, and S. Stringari, Rev. Mod. Phys. **80**, 1215 (2008).  
[7] P. O. Fedichev, Y. Kagan, G. V. Shlyapnikov and J. T. M. Walraven, Phys. Rev. Lett. **77**, 2913 (1996).  
[8] F. K. Fatemi, K. M. Jones and P. D. Lett, Phys. Rev. Lett. **85**, 4462 (2002).  
[9] B. Deb and J. Hazra, Phys. Rev. Lett. **103**, 023201 (2009).  
[10] K. Enomoto, K. Kasa, M. Kitagawa, and Y. Takahashi, Phys. Rev. Lett. **101**, 203201 (2008).  
[11] K. M. Jones, E. Tiesinga, P. D. Lett, and P. S. Julienne, Rev. Mod. Phys. **78**, 483 (2006).  
[12] J. Weiner, V. S. Bagnato, S. Zilio and P. S. Julienne, Rev. Mod. Phys. **71**, 1 (1999).  
[13] B. Deb and G. S. Agarwal, J. Phys. B: At. Mol. Opt. Phys. **42**, 215203 (2009); B. Deb and A. Rakshit, J. Phys. B: At. Mol. Opt. Phys. **42**, 195202 (2009).  
[14] Y. Li, G. Feng, J. Wu, Jie Ma, B. Deb, A. Pal, L. Xiao, and S. Jia, Phys. Rev. A. **99**, 022702 (2019).  
[15] P. G. Burke and K. Smith, Rev. Mod. Phys. **34**, 458 (1962).  
[16] T. Tamura, Rev. Mod. Phys. **37**, 679 (1965).  
[17] J. M. Hutson, Com. Phys. Commun. **84**, 1 (1994).  
[18] T. G. Tiecke, M. R. Goosen, J. T. Walraven, and S. J. J. M. F. Kokkelmans, Phys. Rev. A. **82**, 042712 (2010).  
[19] E. Wille, F. M. Spiegelhalter, G. Kerner, D. Naik, A. Trenkwalder, G. Hendl, F. Schreck, R. Grimm, T. G. Tiecke, J. T. M. Walraven, S. J. J. M. F. Kokkelmans, E. Tiesinga, and P. S. Julienne, Phys. Rev. Lett. **100**, 053201 (2008).  
[20] M. J. Seaton, Proc. Phys. Soc. **88**, 801 (1966); M. J. Seaton, Rep. Prog. Phys. **46**, 167 (1983).  
[21] C. Greene, U. Fano, and G. Strinati, Phys. Rev. A. **19**, 1485 (1979).  
[22] C. H. Greene, A. R. P. Rau, and U. Fano, Phys. Rev. A. **26**, 2441 (1982).  
[23] S. Watanabe and C. H. Greene, Phys. Rev. A. **22**, 158 (1980).  
[24] Z. Idziaszek, A. Simoni, T. Calarco, and P. S. Julienne, New J. Physics. **13**, 083005 (2011).  
[25] S. Watanabe, Phys. Rev. A. **25**, 2074 (1982).  
[26] M. Raoult and G. G. Balint-Kurti, Phys. Rev. Lett. **61**, 2538 (1988).  
[27] M. Raoult and G. G. Balint-Kurti, J. Chem. Phys. **93**, 6508 (1990).  
[28] A. Osterwalder, A. Wuest, F. Markt and Ch. Jungen, J. Chem. Phys. **23**, 11810 (2004).  
[29] J. F. E. Croft, A. O. G. Wallis, J. M. Hutson and P. S. Julienne, Phys. Rev. A. **84**, 042703 (2011).  
[30] F. H. Mies, J. Chem. Phys. **80**, 2514 (1984).  
[31] F. H. Mies and P. S. Julienne, J. Chem. Phys. **80**, 2526 (1984).  
[32] P. S. Julienne and F. H. Mies, J. Opt. Soc. Am. B. **6**, 2257 (1989).  
[33] J. P. Burke, C. H. Greene, and J. L. Bohn, Phys. Rev. Lett. **81**, 3355 (1998).  
[34] F. H. Mies and M. Raoult, Phys. Rev. A **62**, 012708 (2000).

- [35] M. Raoult and F. H. Mies, *Phys. Rev. A* **70**, 012710 (2004)
- [36] B. Gao, E. Tiesinga, C. J. Williams, and P. S. Julienne, *Phys. Rev. A* **72**, 042719 (2005).
- [37] R. Pires, M. Repp, J. Ulmanis, E. D. Kuhnle, M. Weidemüller, T. G. Tiecke, C. H. Greene, B. P. Ruzic, J. L. Bohn, and E. Tiemann, *Phys. Rev. A* **90**, 012710 (2014).
- [38] T. M. Hanna, E. Tiesinga and P. S. Julienne, *Phys. Rev. A* **79**, 040701 (2009).
- [39] J. Hazra, B. P. Ruzic, J. L. Bohn, and N. Balakrishnan, *Phys. Rev. A* **90**, 062703 (2014).
- [40] J. Hazra, Brandon P. Ruzic, N. Balakrishnan, and John L. Bohn, *Phys. Rev. A* **90**, 032711 (2014).
- [41] Z. Idziaszek, T. Calarco, P. S. Julienne, and A. Simoni, *Phys. Rev. A* **79**, 010702 (2009).
- [42] Z. Idziaszek, Z., A. Simoni, T. Calarco, and P. S. Julienne, *New J. Phys.* **13**, 083005 (2011).
- [43] B. Gao, *Phys. Rev. A* **58**, 1728 (1998).
- [44] B. Gao, *Phys. Rev. A* **58**, 4222 (1998).
- [45] B. Gao, *Phys. Rev. Lett.* **104**, 213201 (2010).
- [46] B. Gao, *Phys. Rev. A* **80**, 012702 (2009).
- [47] P. S. Julienne, and B. Gao, *AIP Conf. Proc.* **869**, 261 (2006).
- [48] B. P. Ruzic, C. H. Greene and J. L. Bohn, *Phys. Rev. A* **87**, 032706 (2013).
- [49] Y Cui, C Shen, M. Deng, S. Dong, C. Chen, R. Lu, B. Gao, M. K. Tey and L. You, *Phys. Rev. Lett.* **119**, 203402 (2017).
- [50] M. Li, and B. Gao, *Phys. Rev. A* **86**, 012707 (2012).
- [51] B. Gao, *Phys. Rev. A* **88**, 022701 (2013).
- [52] H. J. Weber and G. B. Arfken, *Essential Mathematical Methods for Physicists* (Academic Press, 2003)
- [53] N. Nygaard, B. I. Schneider and P. S. Julienne, *Phys. Rev. A*, **73**, 042705 (2006).
- [54] E. A. Donley, N. R. Claussen, S. T. Thompson and C. E. Wieman, *Nature*, **417**, 529 (2002).
- [55] T. Köhler, T. Gasenzer, P. S. Julienne and K. Burnett *Phys. Rev. Lett.* **91**, 230401 (2003).
- [56] C. Strauss, T. Takekoshi, F. Lang, K. Winkler, R. Grimm, J. Hecker Denschlag, and E. Tiemann, *Phys. Rev. A*, **82**, 052514 (2010).
- [57] Y. Cui, M. Deng, L. You, B. Gao, and M. Khoon Tey, *Phys. Rev. A*, **98**, 042708 (2018).
- [58] A. Rakshit and B. Deb, *Phys. Rev. A*, **83**, 022703 (2011).
- [59] D. Sardar, S. Naskar, A. Pal, H. Berriche and B. Deb, *J. Phys. B*, **49**, 245202, (2016).
- [60] M. Tomza, K. Jachymski, R. Gerritsma, A. Negretti, T. Calarco, Z. Idziaszek and P. S. Julienne, *Rev. Mod. Phys.* **91** 035001 (2019).
- [61] D. Jaksch, *Contemporary Physics*, **45**, 367 (2004).
- [62] O. Mandel, M. Greiner, A. Widera, T. Rom, T. W. Hänsch and I. Bloch, *Nature*, **425**, 937 (2003).